Műszaki Tudományos Közlemények vol. 18. (2023) 29–36.
DOI: Hungarian: https://doi.org/10.33895/mtk-2023.18.06
English: https://doi.org/10.33894/mtk-2023.18.06

THE STUDY OF THE PROFILE ERRORS OF STRAIGHT TEETHED SHAPER CUTTERS IN THE CAD-ENVIRONMENT

Károly-István GÁL,[1] Márton MÁTÉ[2]

[1] *Sapientia Hungarian University of Transylvania, Faculty of Technical and Human Sciences, Department of Mechanical Engineering, Târgu Mureș, Romania. gal.karoly@ms.sapientia.ro*

[2] *Sapientia Hungarian University of Transylvania, Faculty of Technical and Human Sciences, Department of Mechanical Engineering, Târgu Mureș, Romania. mmate@ms.sapientia.ro*

Abstract

It is well known that straight-teethed shaper cutters present theoretical profile error, which leads to a deviation of the cut gear tooth profile from the involute profile. Taking advantage of the CAD environment, we have visualized and studied shaper cutters at different stages of sharpening. This is advantageous because the effect of any shape or dimension modification of the rake face can be immediately and easily controlled in the design process, thereby saving precious design time.

The aim of our research was to create a 3D model in a CAD environment to visualize different sharpening methods and the profile of shaper cutters at different wear stages, and to estimate the inherent profile errors. The aim of using different sharpening methods was to improve the lateral cutting geometry (especially the lateral relief angle) and also to reduce or – at least – keep the profile error within the accepted limits. During the measurements, both the rake angle and the cutter rack profile angle were changed in order to improve the geometry. The edge was generated using numerically computed points and Autodesk Inventor's special commands. Comparative analyses were performed.

Keywords*: shaper cutter, profile error, CAD, rake face, rake angle, relief engle, cutter rack profile angle.*

1. Basic terminology

1.1. Structure of the classic cutting whee

The Fellow's cutter is essentially a gear with teeth having a rake angle (γ_v) and a relief angle (α_v) [1, 2, 3] as shown in Figure 1.

The rake face is straight circular cone, coaxial with the shaper cutter. Based on the literature, we choose the rake angle $\gamma_v = 5°$ and accept the meshing of it with a straight profile rack type tool which causes profile error [3].

The computing of the profile angle α_s of the Fellow's cutter's meshing rack is based on the approximation presented in the literature [1, 3], where the shaper cutters are considered to have infinite teeth, thus the involute profile is distorted into a straight profile, which causes the profile error.

The tip-relief surface is designed with the use of the characteristic property of involute gears, i.e. profile shifting, which results in a linear decrease of the addendum diameter (*Da*). The profile shifting reaches its maximum in the base plane section (I), is zero in the reference plane II, while plane III reaches its minimum value (ξ_{min}) Plane III also delimits the useful range (*Hh*) of the cutting edge wheel. The total height (*Ht*) is larger than this value to provide the strength and rigidity of the tool [3].

The computing of characteristic circle radii of the cutter is similar to the computing of a cylindrical gear [1–3], thus this calculus is omitted.

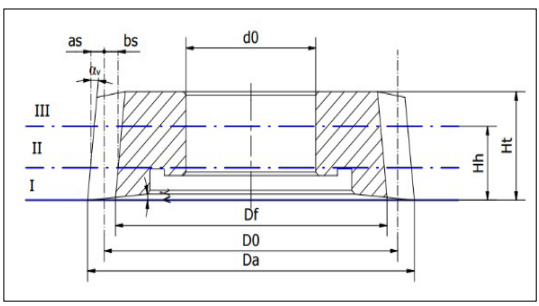

Fig. 1. *Constructive dimensions of the Fellow's cutter.*

1.2. The shape of the side edge

The side edge of the shaper cutter is the intersection of the rake and the lateral relief faces. The equations of the edge [3–6] are written from the parametric equations of the helical involute tooth surface combined in the implicit equation of the conical rake face. In the present communication, we also consider the change in the position of the frontal surface due to re-sharpening. The geometrical relations between the considered surfaces are given in Figure 2.

The position vector of an arbitrary point Q of the side relief surface is given by

$$\overrightarrow{OQ} = \overrightarrow{OG} + \overrightarrow{HG} + \overrightarrow{HQ} \tag{1}$$

whose matrix form related to the frame $Oxyz$ is:

$$\begin{bmatrix} x \\ y \\ z \end{bmatrix} = R_b \begin{bmatrix} cos(\varphi - \eta) \\ sin(\varphi - \eta) \\ 0 \end{bmatrix} + \frac{PE}{2\pi}\varphi \begin{bmatrix} 0 \\ 0 \\ 1 \end{bmatrix} + \tag{2}$$

$$+u \begin{bmatrix} sin\,\beta_b\, cos(\varphi - \eta) \\ -sin\,\beta_b\, cos(\varphi - \eta) \\ -cos\,\beta_b \end{bmatrix}$$

The two chosen parameters for the surface representation are the rotation angle φ of the generating line holding plane while this rolls without slipping on the basic cylinder and the distance u from the point H corresponding to the angle of rotation φ, where the generating line is tangent to the basic helix.

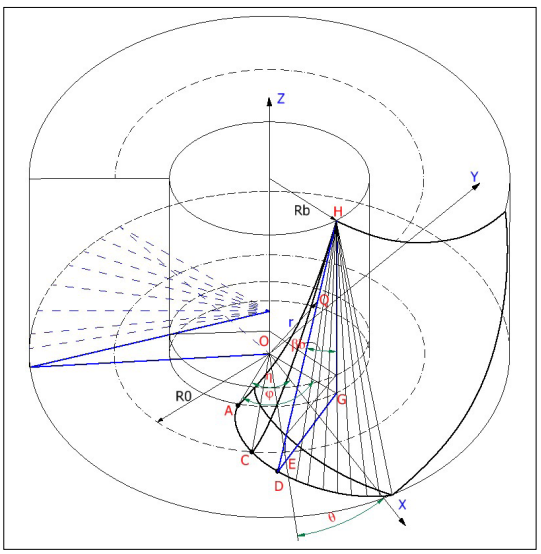

Fig. 2. *Geometric relationships of surfaces.*

The helix parameter can be written as

$$P_E = \frac{2\pi R_b}{tg\ \beta_b}, P = \frac{R_b}{tg\ \beta_b}, tg\,\beta_b = tg\,\alpha_v\, sin\,\alpha_s \tag{3}$$

With the linear transformation $v = u/R_b sin\beta_b$ the equations of the side relief surfaces becomes:

$$\begin{cases} x(\varphi, v) = R_b(cos(\varphi - \eta) + v\, sin(\varphi - \eta)) \\ y(\varphi, v) = jR_b(sin(\varphi - \eta) - v\, cos(\varphi - \eta)) \\ z(\varphi, v) = P(\varphi - v), j \in \{-1; 1\} \end{cases} \tag{4}$$

Note that j = 1 results in the surface shown in Figure 2, while for $j = -1$ it is symmetrical with respect to the Oxz plane.

The angle η s the angle between the polar radius of the base circle point of the involute and the symmetry axis of the complete tooth profile in the Oxy plane, calculated from the second basic equation of evolutionary trigonometry [2]:

$$\eta = \frac{\pi}{2z_s} + 2\frac{\xi_s}{z_s} tg\,\alpha_s + inv\,\alpha_s \tag{5}$$

The geometric interpretation of the angles η and φ is illustrated in Figure 3.

The implicit equation of the rake face, based on Figure 2, is:

$$x^2 + y^2 = (R_a - z\, ctg\,\gamma_v)^2 \tag{6}$$

Assume that due to re-sharpening the rake face moves a distance δ_h talong the z-axis, in its positive direction. Then equation (6) takes the following form:

$$x^2 + y^2 = (R_a - (z - \delta_h)\, ctg\,\gamma_v)^2 \tag{7}$$

From equations (4) and (7), the following relationship between the parameters φ and v results:

$$\varphi(v; \delta h) = \frac{(R_a(\xi s) - R_b \cdot \sqrt{1 + v^2})tg(\gamma_v) + \delta_h}{P} + v \tag{8}$$

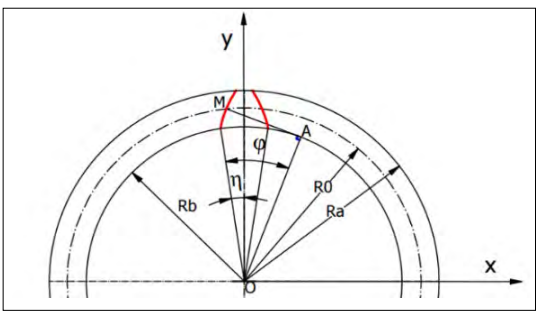

Fig. 3. *Involute's position parameter η and developing parameter ϕ.*

The coordinates of the points on the side edges are given by the coordinate functions (4), with the interparametric dependence (8).

2. Computation of the theoretical profile error

Due to the form of the rake face the tool edge points result one by one from different involutes comprised in different planes perpendicular to the cutter's axis. With increased re-sharpening the profile shifting decreases, thus the points of the implied profiles become closer and closer to the base circle. As a result, the edge form of the shaper cutter changes after each sharpening.

In the main movement, the cutter's edges mesh a gear: this is the equivalent gear of the cutter. Its tooth profile, according to the previous statements and equations (4-8), differs from the involute. The profile error is defined as the difference between the involute tooth profile of a gear with the same number of teeth as the shaper cutter and the tooth profile of the equivalent gear, measured perpendicular to the involute. The latter is referred to in the following as the control profile. The profile error of the cutting wheel can be calculated from the projection of the control profile and the tool edge perpendicular to the *Oxy* plane.

The reciprocate positions of the control profile and the edge projection are shown in **Figure 4**. As can be seen in the figure, the pitch circle points of the control profile and the edge projection coincide. The profile error is positive if the edge projection is outside the control profile and negative if it is inside. As known from **[1–5]**, a positive profile error causes a lightly dedendum undercut of the machined wheel, which ensures an unobstructed connection. Negative profile defects are undesirable as they cause tooth addendum width increasing, which may result in tooth crowding during coupling.

The value of the profile error, for an arbitrary point D of the edge projection equals the length of the segment ED. Its calculation is carried out as shown in **Figure 4.** The selected points of the edge are assumed to be known. Henceforth, we denote by R_b the base radius of the tool involute and by r_b the base radius of the control involute, so that

$$R_0 = \frac{R_b}{\cos\alpha_s} = \frac{r_b}{\cos\alpha_0}.$$

The coordinates of an arbitrary point D of the tool edge projection are (x^D, y^D). Thus:

$$DO = \rho = \sqrt{(x^D)^2 + (y^D)^2} \tag{9.a}$$

$$\angle DOT = \theta = \arccos\frac{r_b}{\rho} \tag{9.b}$$

$$\psi = \operatorname{arctg}\frac{-x^D}{y^D} \tag{9.c}$$

$$\angle COy = \operatorname{arctg}\frac{-x^C}{y^C} \tag{9.d}$$

$$\angle BOT = \theta - \psi + \angle COy + \operatorname{inv}\alpha_0 \tag{9.e}$$

$$ED = DT - ET = \sqrt{\rho^2 - r_b^2} - r_b(\angle BOT) \tag{9.f}$$

To apply the formulas (9.a–f) we need to compute the coordinates of the pitch circle point of the edge projection C. From the equations of the involute curve **[4]**, **Figure 5**.

$$\begin{cases} x(\varphi;\eta) = R_b(sin(\varphi-\eta) - \varphi\, cos\,(\varphi-\eta)) \\ y(\varphi;\eta) = R_b(cos(\varphi-\eta) + \varphi\, sin\,(\varphi-\eta)) \end{cases} \tag{10}$$

we compute the parameter value φ_0 corresponding to the pitch circle:

$$\varphi_0 = \sqrt{\frac{R_0^2}{R_b^2} - 1} = tg\,\alpha_s \tag{11}$$

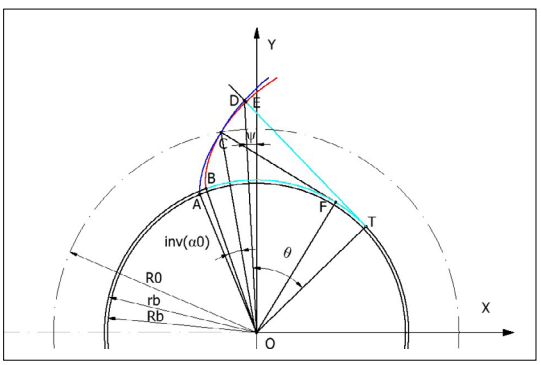

Fig. 4. *Illustration of the edge and control profile.*

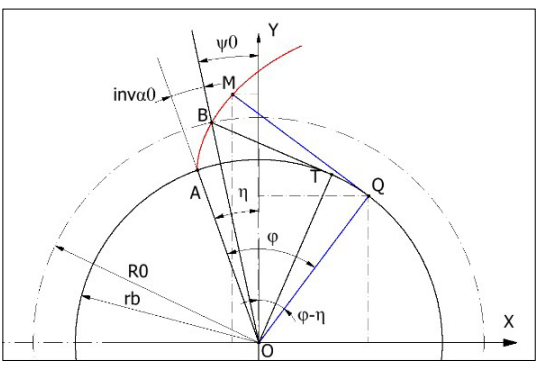

Fig. 5. *Computation of the arbitrary M point of the control involute-*

Thus, the angle between the position vector of point *C* and axis *Oy* is

$$\theta_0 = arctg\frac{x(\varphi_0;\eta)}{y(\varphi_0;\eta)} = inv\,\alpha_s - \eta \qquad (12)$$

A cylindrical helix is started from the point *C* of the tool string, whose parameter *P* is known from (3):

$$\begin{cases} x(w) = R_0 cos\,(\theta_0 + w) \\ y(w) = R_0\,sin(\theta_0 + w) \\ z(w) = Pw \end{cases} \qquad (13)$$

The pitch circle point of the edge is obtained by intersecting the helix given by eq. (13) and the conical rake face. From equations (13) and (7) it follows:

$$R_0^2 = (R_a - (Pw - \delta_h)\,ctg\,\gamma_v)^2 \qquad (14)$$

And from there

$$w_0 = \frac{1}{P}\left((R_a - R_0)\,tg\,\gamma_v + \delta_h\right) \qquad (15)$$

This will give the coordinates of the pitch circle point of the edge projection

$$\begin{cases} x^C = R_0 cos\,(\theta_0 + w_0) \\ y^C = R_0\,sin(\theta_0 + w_0) \\ z^C = (R_a - R_0)\,tg\,\gamma_v + \delta_h \end{cases} \qquad (16)$$

The points of the control profile (16) are calculated using the following equations:

$$\begin{cases} x^M(\varphi) = r_b(sin(\varphi - \eta_0) - \varphi\,cos\,(\varphi - \eta_0)) \\ y^M(\varphi) = r_b(cos(\varphi - \eta_0) + \varphi\,sin\,(\varphi - \eta_0)) \\ \eta_0 = arctg\dfrac{x^C}{y^C} + inv\,\alpha_0 \end{cases} \qquad (17)$$

3. Numerically generated curves

By fitting the equations obtained above into the Mathcad environment, the shaper's involute, the edge curve and the control involute can be plotted with high accuracy.

Equal distanced points are used to represent the curves in order to make the numerical interpolation as accurate as possible. It is a well-known fact [2, 3, 6, 7] that if the running parameter φ of the involute follows an arithmetic progression, then the lengths of the arc-sequences between the points result in a geometric progression. Thus, a linear scaling of φ is not recommended. For equal division, the following computational procedure is used:

– we specify the number of nodes on the considered curve segment;

– calculate the total length of the arc to be divided;

– calculate the arc length of the subdivision;

– iteratively determine the parameter sequence $\varphi_i,\ i \in \overline{0, N-1}$ defining the equidistant nodes.

The elementary involute arc length, according to equations (10), is

$$ds(\varphi) = \sqrt{\dot{x}^2 + \dot{y}^2}\,d\varphi = R_b\varphi d\varphi \qquad (18)$$

The interval of the parameter φ fits:

$$\sqrt{\frac{R_t^2(\xi_s)}{R_b^2} - 1} \le \varphi \le \sqrt{\frac{R_a^2(\xi_s)}{R_b^2} - 1} \qquad (19),$$

where $R_t^2(\xi_s)$ and $R_a^2(\xi_s)$ are the involute root radius and the addendum radius corresponding to the maximum tool profile shifting value, respectively.

Denote the corresponding parameter values by φ_t and φ_a respectively. The total length of the involute arc, by integrating the arc length (18) is

$$L = \int_{\varphi_t}^{\varphi_a} d\varphi = \frac{1}{2}R_b(\varphi_a^2 - \varphi_t^2) \qquad (20)$$

The *N* arc points determine *N*−1 involute-arc segments of equal length ΔL = L/(N−1). This is used to construct the corresponding parameter sequence, with the following recursion:

$$\varphi_0 = \varphi_t,\ \Delta L = \int_{\varphi_j}^{\varphi_{j+1}} d\varphi,\ j \in \{0,1,\ldots,N-2\} \qquad (21)$$

After computing we obtain the following series:

$$\varphi_{j+1} = \sqrt{\frac{2\Delta L}{R_b} + \varphi_j^2}, j \in \{0,1,\ldots,N-2\} \qquad (22)$$

Figure 6 shows N=13 equidistant points of the involute of a shaper cutter with z_s=27 teeth and m=3.75 mm module, while the tooth surface – a helical involute – is shown in **Figure 7.** Here also

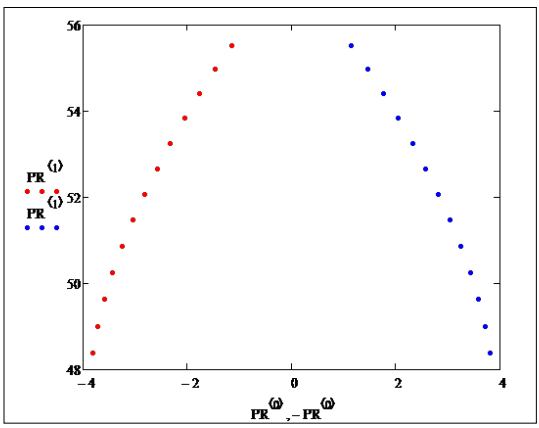

Fig. 6. *Equally distanced shaper involute points.*

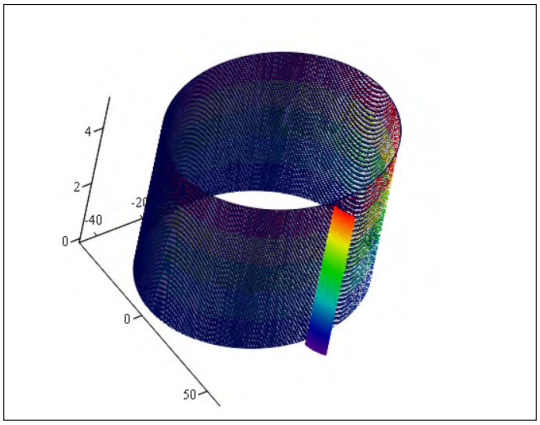

Fig. 7. *Tool tooth surface built on the involute.*

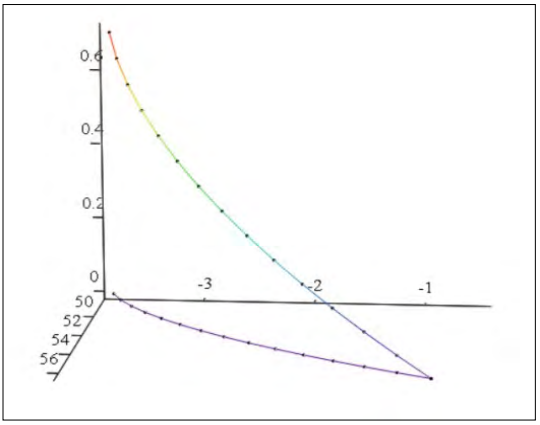

Fig. 8. *Equidistant divided tool edge curve and its projection.*

was considered the same equidistant division of the involute, with the control of the v parameter limits in such manner that the surface points fall between the two limiting planes of the cutter. Using the 3rd of equations (4), for each value of φ, the limits of v can be computed.

The profile shifting factor ξ, as a function of the tool wear value δ_h, influences the shape and the limits of the edge curve.

Figure 1 shows that the translation of the rake face cone by δ_h causes a displacement of the same amount of the tooth basic plane, so that we have to expect a $\Delta R_a = \delta_h \operatorname{tg} \alpha_v$ addendum radius decrease. Due to the linear relationship between the addendum radius and the profile shift, this determines a profile shift decrease of $\Delta\xi = \Delta R_a / m$ Thus, the tool profile shifting value corresponding to δ_h becomes

$$\xi(\delta_h) = \chi = \xi s - \frac{\delta h \cdot tan\,(\gamma v)}{m} \qquad (23)$$

Accordingly, the integration limits in formula (19) will change.

For the tool edge curve, the expression of the elementary arc length in (18) is much more complicated than in the case of the involute. The complicated computational formulae would introduce significant rounding error anyway, so we start the side-edge subdivision from the equidistant subdivision of the base involute, assuming that it will not differ significantly from the equidistant subdivision due to the specific geometry of the rake face and the low rake angle value. Therefore, we assign to each of the nodes of the basic plane involute a helix of parameter P that fits the side relief face. The edge points result as intersection points of the twist line and the rake face.

The polar coordinates of the j^{th} member of the point series generated by formula (22), in correspondence with the involute geometric properties, are polar radius

$\rho_j = R_b\sqrt{1+\varphi_j^2}$, and polar angle

$\theta_j = -\eta + \varphi_j - \operatorname{arctg}\varphi_j$, The equations of the twist line from here can be written, in formal identity with equations (13). On the basis of (15), the value of the v parameter, for each j, results as

$$w_j = \frac{1}{P}\left(\left(R_a - \rho_j\right) tg\,\gamma_v + \delta_h\right) \qquad (24)$$

The edge curve calculated for the previous numerical example is illustrated in **Figure 8**.

4. CAD model in Autodesk Inventor environment

4.1. Construction of the body model

The body model is built on four involute curves created in parallel planes arranged in descending order of profile shifting. These are defined for $\xi \in \{0{,}3;\ 0;\ -0{,}3;\ -0{,}605\}$. Since the tooth surface of the tool is a helical involute surface, we computed their initial angle η. The height of the planes above the basic plane xOy was calculated using the formula given in **[3]**

$$h_i = (\xi_s - \xi_i)\, m\, ctg\, \alpha_v \qquad (25)$$

The projections of the four involutes in the xOy plane are illustrated in **Figure 9.** The generated involutes were connected using the Autodesk Inventor command „Loft". After realizing one tooth this was extended to obtain the 3D model of the shaper cutter **[8]** (**Figure 10**).

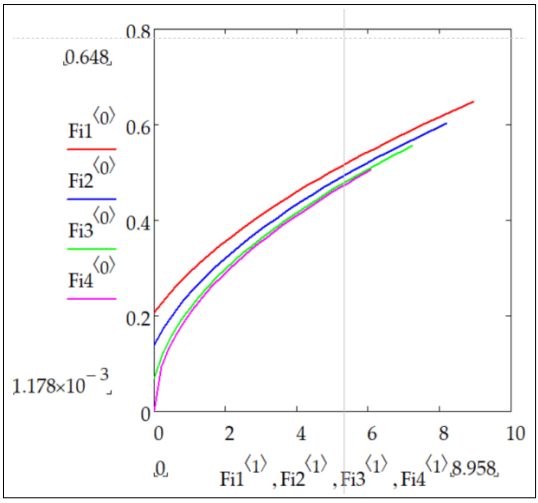

Fig. 9. *Illustration of involutes with different profile shifts.*

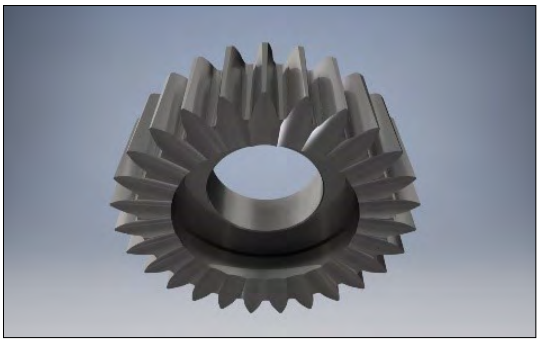

Fig. 10. *Shaper cutter 3D model.*

4.2. Function of the model

With the model, any attempt to modify both the shape and the dimensions of the rake face can be immediately and easily checked in the design process, saving precious time. Secondly, different sharpening methods and sharpening stages can be predicted, which facilitates both the design process and the prediction of the tool parameters and, based on this, the accuracy of the gears produced with a given tool. The model allows the inspection of the distribution and the maximum value of the theoretical profile error in a graphical environment.

5. Case study

Two profile error analysis methods have been developed in a CAD environment:

Method I.: in this case, the numerically generated equivalent gear involute was implemented in Autodesk Inventor and the tool edge was developed in Inventor using the specific commands of the software.

The measurement method comprised the following steps:

Intersection of the model body with the rake face. Classical conical surface, common for all teeth, or individual rake face for each tooth, can be here adopted.

Graphical output of the edge curves.

Projection of the edge curves in the plane xOy perpendicular to the axis.

Adding of the involute profile of the equivalent gear (number of teeth and module of the shaper cutter but the rack profile angle α_0) to the projection curve, ensuring the overlap of pitch circle points of both.

Now the two curves plotted before will be intersected by a tangent line to the basic circle of the equivalent gear.

The profile error equals the length of the segment cut by the two curves.

Measurements were taken on the involute inner circle (R_t) and head circle (R_a) of the Fellow's cutter.

In our study, several sharpening stages were simulated and two sharpening methods were simultaneously analyzed: classical conical sharpening and cylindrical surface sharpening [8]. The variation of the errors was studied for the variation of the rack profile angle, the sharpening stage and the rake angle. The results obtained are presented in Tables 1–4.

Table 1. *Measured profile error values, for conical rake face*

Cases	R_t [mm]	R_a [mm]
α_s, $\xi = 0.3$	0.005	0.021
α_s+10', $\xi = 0.3$	0.001	0.004
α_s−10', $\xi = 0.3$	0.015	0.033
α_s, $\xi = 0$	0.008	0.015

Table 2. *Measured profile error values, for cylindrical rake face*

Cases	R_t [mm]	R_a [mm]
α_s , $\xi = 0.3$	0.001	0.008
α_s+10', $\xi = 0.3$	0.007	0.012
α_s−10', $\xi = 0.3$	0.011	0.016
α_s , $\xi = 0$	0.003	0.003

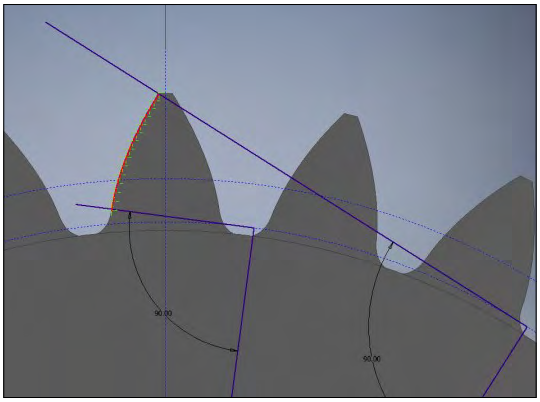

Fig. 11. *Profile error measurement Case I.*

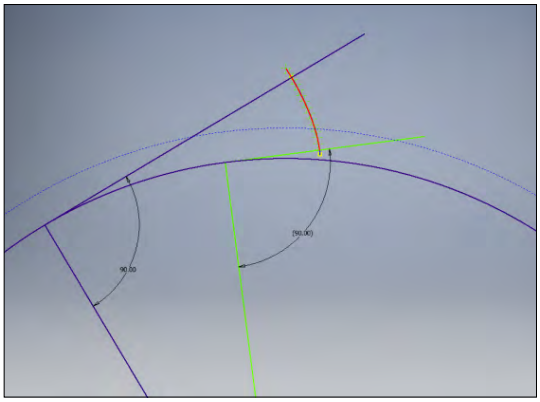

Fig. 12. *Profile error measurement Case II.*

In **Table 1** the theoretical profile error of a new shaper cutter with maximum profile shifting is shown, considering a classical circular cone rake face with $\gamma_v = 5°$. The tool's rack profile angle is set to $\{\alpha_s - 10'; \alpha_s; \alpha_s + 10'\}$ In the last row of the table, the errors were investigated for the nominal value of α_s, but for a tool profile shifting of $\xi = 0$.

In the second table, the error values were obtained in the case of applying a cylindrical rake face for each tooth. The parameters of the cylinder are radius $\rho_h = 12$ mm, and the axis inclination angle 5°.

Method II.: in this case, both the equivalent gear involute and the tool edge projection curve were numerically obtained and after that implemented in Autodesk Inventor, where and measurements were performed. In this way, we eliminated the need to build a spatial model.

Table 3. *Method II., errors on the involute inner circle*

α_s	$\gamma_v = 5°$	$\gamma_v = 10°$	$\gamma_v = 17°$
$\delta_h = 0$ mm	0.006	0.014	0.023
$\delta_h = 5$ mm	0.007	0.013	0.023
$\delta_h = 10$ mm	0.007	0.014	0.023
$\delta_h = 20$ mm	0.007	0.014	No data

Table 4. *Method II., errors on the addendum circle*

α_s	$\gamma_v = 5°$	$\gamma_v = 10°$	$\gamma_v = 17°$
$\delta_h = 0$ mm	0.019	0.038	0.066
$\delta_h = 5$ mm	0.017	0.032	0.049
$\delta_h = 10$ mm	0.016	0.026	0.033
$\delta_h = 20$ mm	0.012	0.015	No data

The measurement procedure is similar to the method outlined in Case I., except that both the control profile and the edge curve were generated numerically (**Figure 12**).

The second measuring method was used only for the case of conical rake face. We investigated the variation of the profile errors for several stages of tool wear and for a constant value of the tool's generating rack profile angle α_s.

6. Conclusions

The distribution of the errors differs from the results obtained using the pure mathematical investigation model. As illustrated in **Figure 3,** the projection of the tool edge is tangent to the control profile on the pitch circle and is located outside it. In contrast, in the Autodesk Inventor environment, in 95% of the cases, we found that only the edge projection segment between the pitch circle and the addendum circle is located outside of the control profile. The section between the involute inner circle and the pitch circle fits within the control profile in the majority of cases. Results of the present study show that the relative position of the two curves fits the mathematical model only for the case of α_s+10°, ξ(0.3) and conical rake face; however, in this case the profile error was found to be the smallest.

Looking at the results of cases I and II, it can be said that changing the tool generating rack profile angle is not advantageous in all cases for profile error evolution.

Changing the classical literature-based tool rack profile angle was useful in only one case, as it is supported by the obtained results; otherwise, increasing or decreasing it leads to an increase in the profile errors in most cases.

The investigation of the cylindrical rake face proved to be effective. The profile errors on the addendum circle were significantly smaller than those arising by the use of the conventional rake face.

With increases in rake angle γ_v the profile error gradually increases, but the chip removal capability is greatly improved. Our measurements show an increasing trend from the inner involute circle to the addendum circle.

Too high a rack angle value is detrimental to the tool-life because the possible number of re-sharpening decreases drastically.

As δ_h increases, the profile error on the involute inner circle remains constant, while it gradually decreases on the addendum circle.

References

[1] Hollanda D.: *Aşchiere şi scule.* Reprografia I. I. S. Tg. Mureş, 1994. 234–240.

[2] Szeniczei L.: *Az általános fogazás.* Nehézipari Műszaki Könyvkiadó, Budapest, 1958. 49–50.

[3] Máté M.: *Hengeres fogaskerekek gyártószerszámai.* Erdélyi Múzeum-Egyesület, Kolozsvár, 2016. https://doi.org/10.36242/mtf-12

[4] Máté M.: Az egyenesfogú metszőkerék szerszámkapcsolószögének optimálása. Műszaki Tudományos Füzetek – FMTÜ I. sz. (1996) 12–15. https://doi.org/10.36243/fmtu-1996.03

[5] Máté M., Kántor A., Laczkó-Benedek B.: *Metszőkerékkel lefejtett fogaskerekek profilpontosságának vizsgálata.* Műszaki Tudományos Közlemények, 7. (2017) 279–282. https://doi.org/10.33895/mtk-2017.07.62.

[6] Máté M., Hollanda D.: *Az egyenesfogú metszőkerék geometriai modell számítógépes kiértékelésének hibái.* Műszaki Tudományos Közlemények, 10. (2019) 53–58. https://doi.org/10.33894/mtk-2019.10.06

[7] Máté M., Hollanda D., Tolvaly-Rosca F., Forgó Z., Egyed-Faluvégi E.: *Synthesis of a Profile Errorless Involute Shaper Cutter with Cylindrical Rake Face.* In: 2019 IEEE 19th International Symposium on Computational Intelligence and Informatics and 7th IEEE International Conference on Recent Achievements in Mechatronics, Automation, Computer Sciences and Robotics (CINTI-MACRo), Szeged, 14–16 November 2019. 71–76. https://doi.org/10.1109/CINTI-MACRo49179.2019.9105302

[8] Tolvaly-Roşca F.: *A számítógépes tervezés alapjai: AutoLisp és Autodesk Inventor alapismeretek.* Erdélyi Múzeum-Egyesület, Kolozsvár, 2009. https://doi.org/10.36242/mtf-07